Available online at www.sciencedirect.com

ScienceDirect

Procedia - Social and Behavioral Sciences 120 (2014) 496 – 505

Procedia
Social and Behavioral Sciences

The 3rd International Geography Symposium - GEOMED2013

Bank erosion and secondary circulation in a meandering laboratory flume

Donatella Termini*

Dipartimento di ingegneria Civile, Ambientale, Aereospaziale, dei Materiali (DICAM) – University of Palermo - Viale delle Svienze – 90128 Palermo (Italy)

Abstract

This paper reports peculiar results of experimental investigation on the secondary circulation motion of flow along a meander wave. Experiments were conducted in a large amplitude meandering laboratory channel for two values of the width-to-depth ratio. Here attention is focalized on how secondary motion affects the bank shear stress distribution, influencing the stability of the outer bank. The analysis essentially highlights that, especially for small width-to-depth ratio, as the channel curvature increases, besides the classical central-region secondary circulation cell a counter-rotating circulation cell forms in the outer-bank region. Such counter-rotating circulation cell allows the bank shear stress to obtain small values at the outer bank.

Keywords: Open-channel flow; meander wave; secondary motion; bank stability.

1. Introduction

A large amount of experimental research on secondary flow motion in bends has been performed.

Studies conducted in constant curved channels have highlighted the formation of an unique secondary circulation cell in the central-region of the cross-section (Kikkawa et al., 1976; Zimmerman & Kennedy, 1978). This circulation

* Corresponding author. Tel.: +39-091-238-96522; mobile: +39-3287274471 ; fax: +39-091-238-60810
E-mail address: donatella.termini@unipa.it

1877-0428 © 2013 The Authors. Published by Elsevier Ltd.
Selection and peer-review under responsibility of the Organizing Committee of GEOMED2013.
doi:10.1016/j.sbspro.2014.02.129

cell tends to move the maximum flow velocity at the outward side of the bend leading to a strong attack of the outer bank.

But, other studies conducted in natural channels (Bathurst et al., 1979; Dietrich & Smith, 1983) and results recently obtained by Blanckaert and Graf (2001) in a strongly constant curved laboratory channel (for small width-to-depth ratio: B/h=3.6<10), have shown that, besides the central-region circulation cell, a small and weak counter-rotating circulation cell develops near the free surface of the outer bank of the bend.

Furthermore, recent investigations (Termini, 2004; Termini & Piraino, 2007) on cross-sectional flow motion at the apex section of a large amplitude meandering laboratory channel (for small width-to-depth ratio: B/h=9<10) have also highlighted the formation of the central-region and outer-bank secondary circulation cells.

Thus, in reality, it seems that, for small width-to-depth ratio, the secondary flow motion in bends may be obtained by the combination of the classical central-region circulation cell and of the aforementioned counter-rotating circulation cell developing near the outer bank. The presence of the counter-rotating circulation cell could influence the bank shear stress distribution and, thus, it may be of crucial importance for the bank stability (Blanckaert & Graf, 1999; Termini & Piraino, 2008).

The aim of the present work is to give a contribution on the evolution pattern of both the circulation cells along a meander wave for two values of the width-to-depth ratio (>10 and <10).

Nomenclature

B	channel width
g	acceleration of gravity
h	water depth
Q	water discharge
r	transversal abscissa
R	radius of curvature at the channel axis
R_h	hydraulic radius of the cross-section
S	longitudinal channel slope
u_*	shear velocity
U	average flow velocity
v_r	radial velocity component
$\overline{v_r}$	depth-averaged value
v_r^*	local deviation of radial velocity component
v_z	vertical velocity component
z_b	local bed elevation
z_{sur}	local free surface elevation
v_r'	instantaneous fluctuation component in direction r
v_s'	instantaneous fluctuation component in direction s
σ_g	standard deviation
τ_{rs}	bank shear stress
τ_N	normalized bank shear stress
ψ	streamline function
ψ_r	depth-averaged streamline function – radial direction
ψ_z	depth-averaged streamline function – vertical direction
ψ_N	normalized streamline functions

2. Experimental setup

Experiments were performed in a meandering laboratory channel that follows the sine-generated curve with a deflection angle of 110°. The plane view of the experimental installation is reported in Figure 1a. The channel is constructed at the Dipartimento di Ingegneria Civile, Ambientale, Aerospaziale, dei Materiali - University of Palermo (Italy). The channel cross-section is rectangular with width B=0.50 m; the banks are rigid and the bed is of quartz sand, with medium sediment diameter of 0.65 mm and geometric standard deviation σ_g=1.34. Details of the experimental installation can be found in previous works (Termini, 2004; Termini & Piraino, 2007).

A first mobile-bed run was conducted until the equilibrium bed topography was reached. The initial longitudinal bed slope at the channel axis was S=0.371% and the water discharge was Q=0.012 m3/s. At the end of such run the deformed bed was fixed by using cement dust. Then, other two runs were conducted: one (run 1) with the same water discharge (Q=0.012 m3/s) and the other one (run 2) with water discharge of 0.007 m3/s. The corresponding overall-averaged water depths were respectively equal to h=0.055 m (width-to-depth ratio equal to 9.0) and to h=0.03 m (width-to-depth ratio equal to 16.7).

During each run the local longitudinal, radial and vertical flow velocity components were measured by using an Acoustic Doppler Velocity Profiler (DOP 2000), by Signal Processing s.a., as described in previous works (Termini & Piraino, 2007; 2008). The measures were carried out in 33 sections, opportunely selected along the channel. In this work the analysis is restricted to sections A÷E reported in Figure 1b.

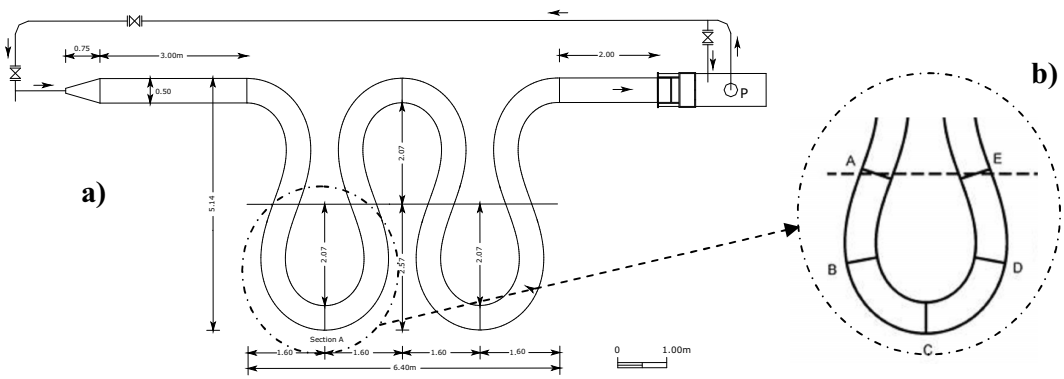

Fig. 1. (a) plane view of the experimental apparatus; b) measurement sections

3. Cross-sectional flow motion

3.1. Radial and vertical velocity distributions

In order to analyze the evolution of secondary flow motion along the examined channel reach, which is included between the two inflection sections A and E, the distributions of measured radial (v_r,) and vertical (v_z) velocity components have been determined in each considered section. Figures 2 and 3 report, respectively, the vector representations of v_r and v_z at the characteristic sections A, B, C, D, E.

In these figures three regions can be identified for each section: the inner-bank region (r<10), the central region (10<r<42) and outer-bank region (r>42).

In particular, from Figure 2 it can be observed that: in the inflection section A, especially for B/h<10, all vectors v_r are directed toward the inner bank (negative versus) both in the inner-bank region and in the central region, with exception of a thin area of the central region where the vectors change the sign near the bed. This behavior could be due to the local bed deformation. In the outer-bank region, all vectors v_r are directed toward the outer bank (positive

versus), probably because of the influence of the inflow conditions. In case of B/h>10 (run 2) no reliable data have been obtained in the outer-bank region. As the channel curvature increases (section B), all v_r vectors are directed towards the outer bank (positive versus) for both the B/h ratios. At apex section C, and in the case of B/h<10, v_r changes again the sign and, both in the inner-bank region, (where deposition occurs) and in the major part of the central-region, all vectors are directed towards the inner-bank (negative versus). Approaching the outer-bank region the vectors v_r change in sign along the measurement verticals so that near the free surface they are directed towards the outer bank (positive versus) and near the bed they are towards the inner bank. In case of B/h>10, the crossed trend of the vertical profiles of v_r occurs only in the central region (approximately at r»B/2); then, approaching the outer bank, the versus of all vectors v_r is positive while approaching the inner bank the versus of all vectors v_r is negative.

As the channel curvature decreases, i.e. passing from section C to section D, the crossed vertical profiles of v_r are found both in the central region and very close to the outer bank for run 1 (B/h<10). For run 2 (B/h>10), the crossed vertical profiles are found only in the outer-bank region, where the higher values of water depths occur. Finally, in the inflection section downstream (section E), the radial velocity vectors are all directed toward the inner bank for both the considered B/h ratios.

Thus, it can be concluded that, especially for B/h<10, as the channel curvature increases, crossed vertical profiles of v_r occur near the outer bank

From Figure 3 it can be observed that: in the inflection section A all vectors v_z are directed towards the bed (negative versus), for B/h<10. In case of B/h>10 (run 2), in the inner-bank region the vectors v_z are directed towards the free surface (positive versus); in this case, no reliable data have been obtained in the outer-bank region. In section B, for B/h<10, v_z are generally towards the bed (negative versus) both in inner-bank and in central regions, although in some thin areas v_z changes the versus (especially near the bed of the central-region); in the outer-bank region the vectors v_z are all directed towards the free surface (positive versus) with exception of a thin area near the free-surface where they assume negative versus.

In case of B/h>10, both in inner-bank and in central regions, all vectors v_z are towards the bed (negative versus); in the outer-bank region the vectors v_z change in versus At apex section C, for both the B/h ratios, in the major part of the central-region and in part of the outer-bank region, the vectors v_z change the versus passing from the free-surface (where the versus is negative) to the bed (where the versus is positive). This behavior is more evident for B/h<10. As the channel curvature decreases (section D), the crossed vertical profiles of v_z especially occur near the outer-bank. Finally, in the inflection section downstream (section E), all vectors v_z are directed towards the bed (negative versus), except in part of the central region and near the outer-bank where they become positive (toward the free-surface) near the bed. It can be concluded that, also for v_z crossed vertical profiles can be observed near the outer bank, where erosion occur.

3.2. Cross-flow streamlines

The cross-stream flow is determined by the combination of the radial and vertical velocity components. According with previous researchers (Bachelor, 1967; Bradshaw, 1987; Blanckaert et al., 2008), in order to separate the contribution of the cross-stream circulation from that of the average convective transport motion, the local radial flow velocity component has been decomposed into the sum of the depth-averaged value, $\overline{v_r}$, and of its local deviation, v_r^*:

$$v_r = \overline{v_r} + v_r^* \tag{1}$$

The component $\overline{v_r}$ produces a net flux of mass in transverse direction. In a previous work conducted by using the same experimental data as in the present work, Termini & Piraino (2011) observed that, at the crossover (i.e. for the considered case, at inflection sections A and E), where the cross-circulation component is negligible, the net transversal flux of mass is always towards the inner-bank; at the entrance of the downstream

bend (i.e. for the considered case, at section B) it is observed that, very close to the outer-bank where the formation of a counter-rotating circulation cell could initiate, the net transversal flux of mass changes the sign and it is towards the outer bank. At the bend apex (i.e. for the considered case, at section C), the transversal flux of mass is towards the inner bank in the inner region, where the water depths are low and the cross-circulation is negligible; in the central region of the cross-section, where the effect of the central circulation cell dominates, the net transversal flux of mass assumes very low values until that, in the outer bank region where the water depths are high, the transversal flux of mass increases in value and it is towards the outer bank. But, because of the formation of the counter-rotating circulation cell, very close to the outer bank the net transversal flux of mass rapidly decreases in value, eventually changing the sign depending on the strength of the counter-rotating cell itself.

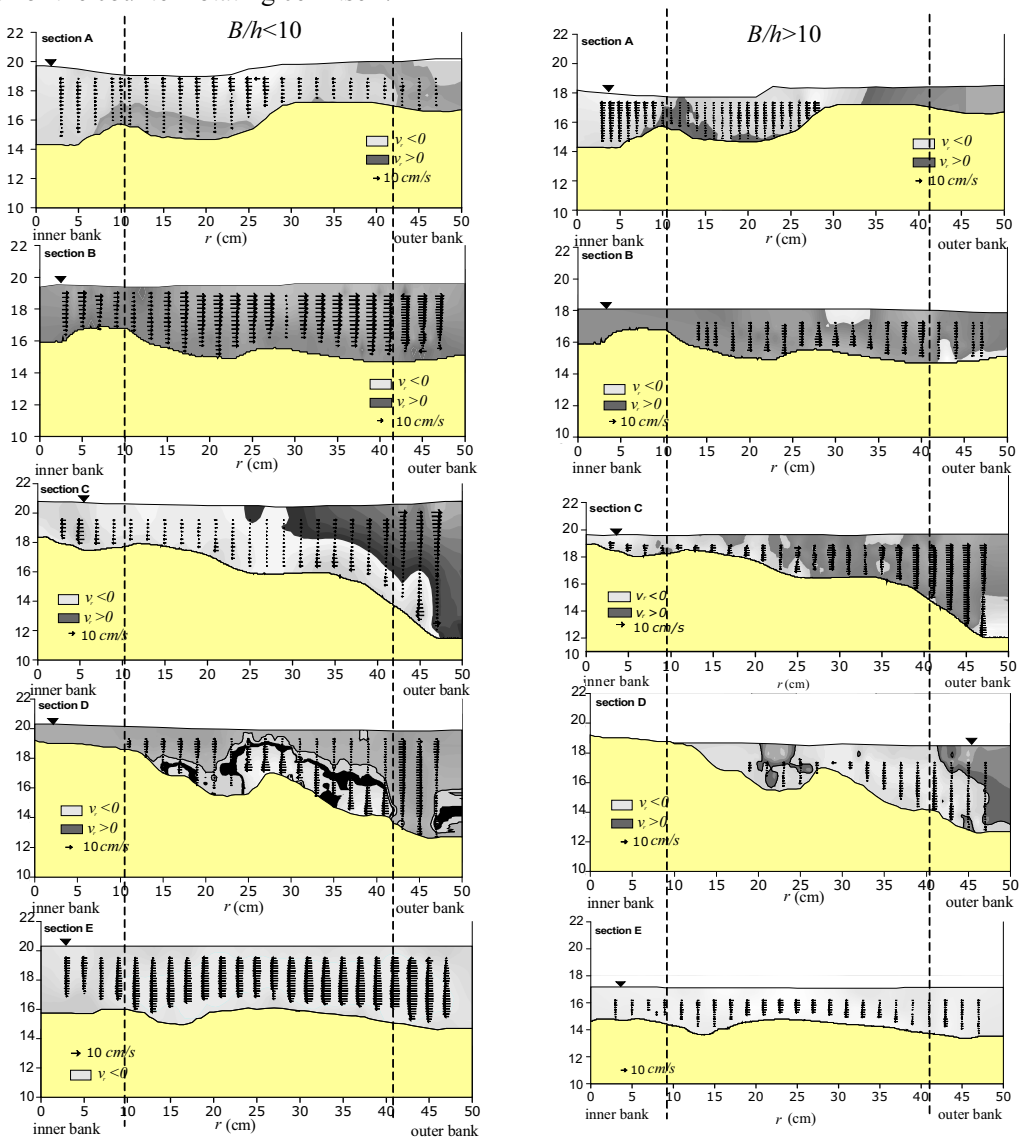

Fig. 2. Distributions of transverse flow velocity component

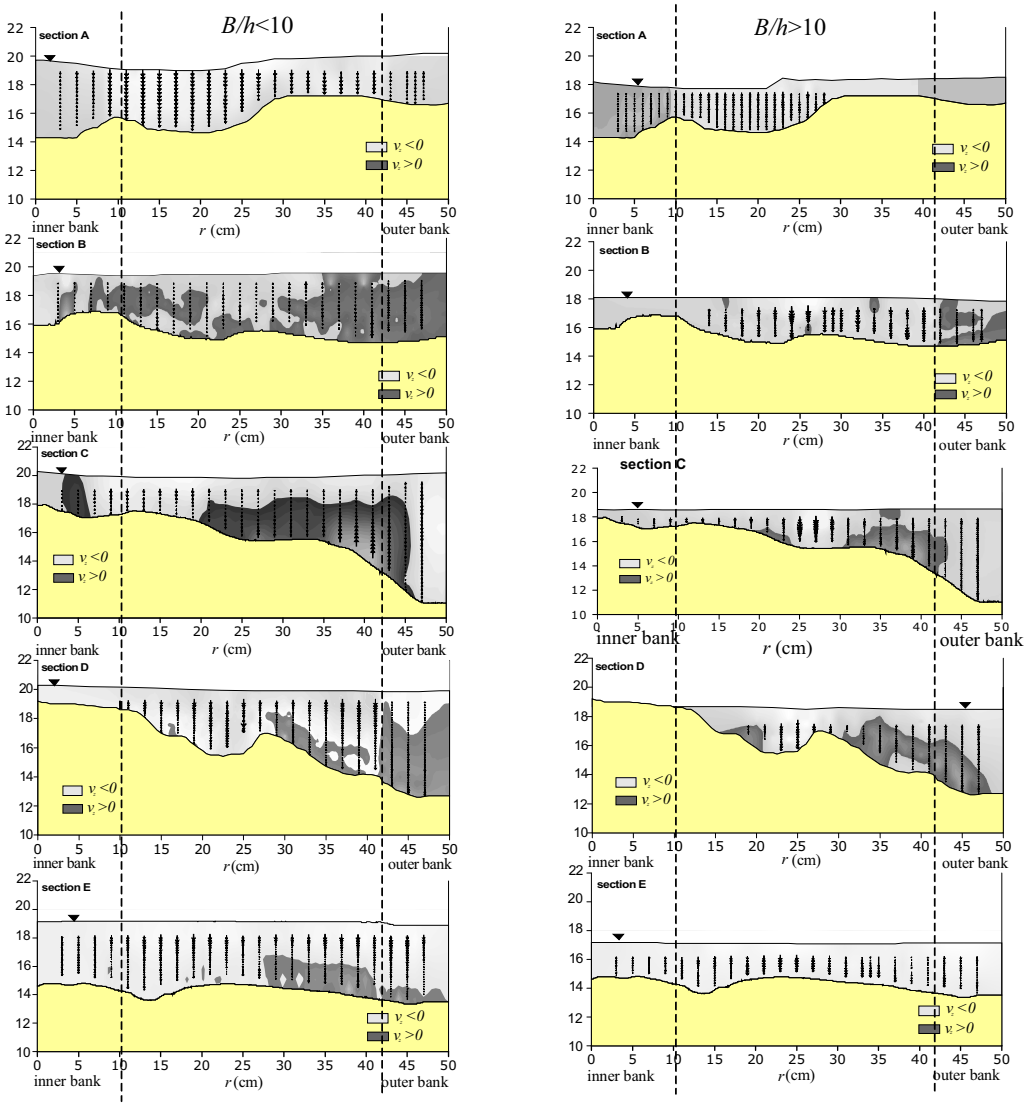

Fig. 3. Distributions of vertical flow velocity component

This already indicates that the cross-circulation and the advective momentum transport by cross-stream flow play an important role in the bed and bank erosion processes.

The cross-stream circulation is determined by the combination of v^*_r and v_z. It can be visualized through the streamline function ψ, which is defined as (Blanckaert et al., 2008):

$$\psi = \frac{1}{2}\left(\psi_r + \psi_z\right) \tag{2}$$

with: $$\psi_r = -\left(1+\frac{r}{R}\right)\int_{z_b}^{z_{sur}} v_r^* \, dz \qquad \psi_z = \int_{-B/2}^{r}\left(1+\frac{r}{R}\right) v_z \, dr + cte \tag{3}$$

where r is the local radius of curvature, R is radius of curvature at the channel axis (being the term $1+r/R$ a metric factor), z_b and z_{sur} are the local bed and free surface elevations, respectively; the integration constant in Eq. (3) is chosen so that the cross-sectional averaged values of ψ_r and ψ_z are equal (Blanckaert et al., 2008). In Figure 4 the contour-lines of normalized streamlines functions $\psi_N = (100\psi/(Uh))$, with $U=Q/Bh$, are reported for both the considered width-to-depth ratios.

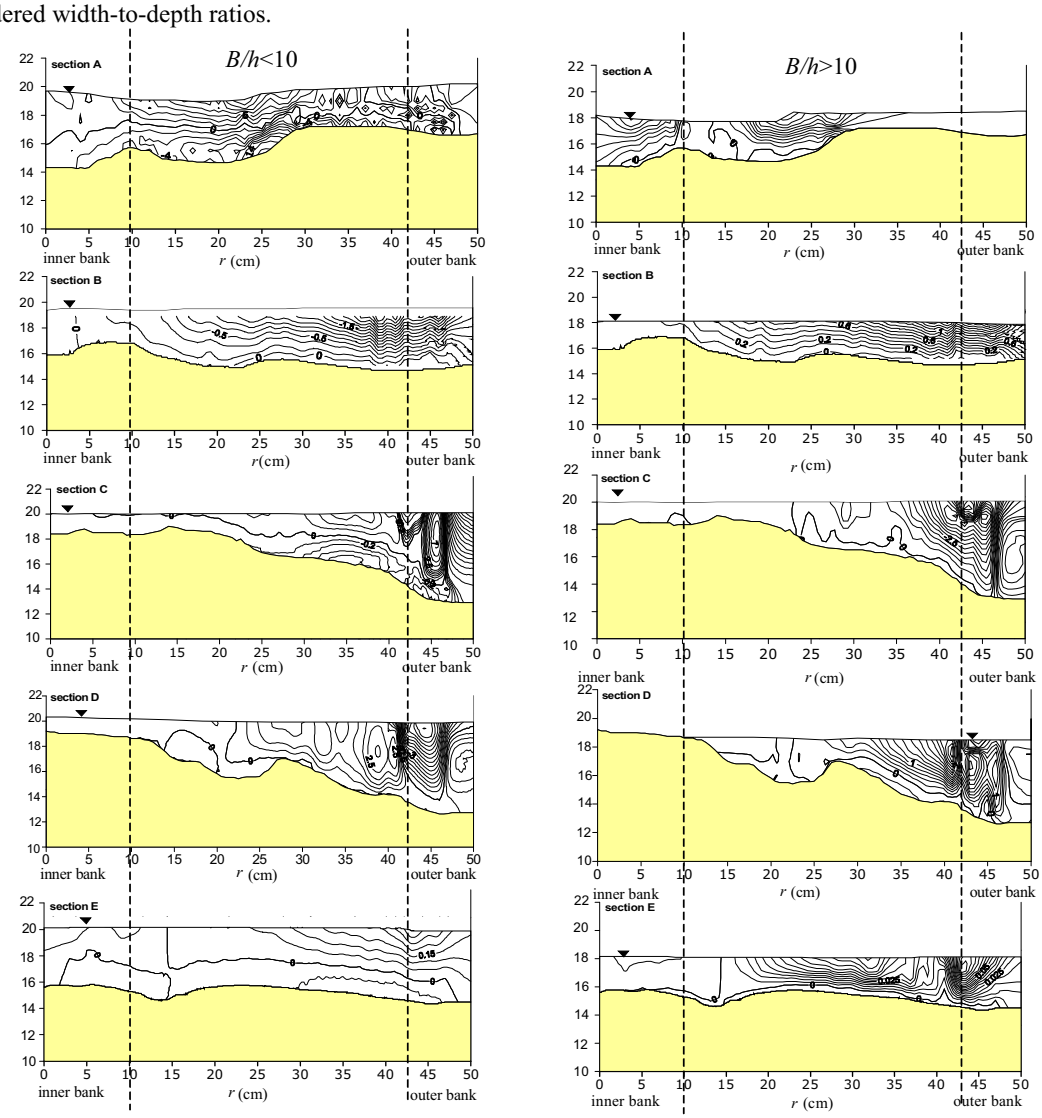

Fig. 4: Contour-lines of stream-line function

Figure 4 shows that in section A, for both the *B/h* ratios, the streamlines do not show evident circulation cells. In section B, the ψ_N patterns are in general rather smooth, but, in case of *B/h*<10, it can be observed that the contour-lines thicken near the free surface of the outer bank. At the apex section C, three circulation cells seem to form in the case of *B/h*<10: in the outer-bank region a first circulation cell (with negative values of ψ_N) occurs near the free surface; a second circulation cell (with positive values of ψ_N) seems to form close to the outer-bank; a third circulation cell (with positive values of ψ_N) forms in the central region (but shifted toward the outer-bank region).

Finally, in the inflection section downstream (section E), for both the width-to-depth ratios, the contour lines are again smooth, except that in a thin area of the outer-bank region, as observed in the previous section A.

Thus, the observed ψ_N patterns seem to highlight the formation of a secondary counter-rotating circulation cell that initiates approximately at the bend entrance (section B); then it evolves until to reach the apex section (section C) and decays at the bend exit (section D). This behaviour has been especially observed in the case of *B/h*<10.

4. Distribution of bank shear stress

In order to analyze how the cross-sectional flow motion, observed for *B/h*<10, affects the bank erosion, the distribution of the bank shear stress $\tau_{rs} = -\rho\overline{v'_r\, v'_s}$ (where v'_i - *i=r, z, s* - represents the instantaneous fluctuation component in direction *i;* the over-bar indicates the time-averaged value) has been estimated in each examined section.

In Figure 5 the horizontal profiles of the normalized bank shear stress, $\tau_N = -\tau_{rs}/\rho u_*^2$ (with $u_* = \sqrt{gR_hS}$ - *g* is the acceleration of gravity, R_h the hydraulic radius of the cross-section), are reported for sections A÷D. In this figure, *z* indicates the water level with respect to an horizontal reference plane.

Figure 5 shows that in section A the values of τ_N weakly increase approaching to the outer-bank. Then, in section B, near the outer bank τ_N changes the sign; the higher negative values of τ_N are found at 38<*r*<45. At the apex section C a high negative value of τ_N is found at 38<*r*<40, but approaching the outer bank τ_N changes again the sign assuming a peak positive value at *r*=45 cm. Then, it decreases assuming very low values close to the outer bank. Similar behaviour of τ_N can be observed in section D, but here the peak positive value of τ_N is strongly reduced.

5. Downstream velocity distribution

The effect of the momentum transport of cross-sectional motion on the downstream velocity redistribution can be examined through Figure 6. This figure reports the distribution of the normalized depth-averaged streamline function, $<\psi_N>= (100<\psi>/(Uh))$ (in Figure 6a) and the distribution of the depth-averaged longitudinal flow velocity, v_s , (in Figure 6b). As Figure 6a shows, $<\psi_N>$ gradually increases passing from section A to section C. At section C, the maximum of $<\psi_N>$ is found in the outer-bank region but not very close to the outer bank itself; at the bend exit (section D) the maximum increases in value and slightly moves towards the outer bank; then $<\psi_N>$ decreases in value until to reach the crossover section downstream.

Figure 6b highlights that the maximum v_s lies, at the bend entrance, near the inner bank. Then, it moves towards the outer bank. Along the channel reach B – C the maximum of v_s further shifts towards the outer bank but it maintains at a certain distance from the outer bank itself, because of the presence of counter-rotating circulation motion near the outer bank. Passing from section C to section D, where the counter-rotating circulation cell extends towards the bed and the function $<\psi_N>$ assumes the higher value, the maximum of v_s tends to slightly move towards the central region of the cross-section. Then, along the reach D-E, where the counter rotating cross-circulation decays, v_s decreases in value and the maximum is found at the outer bank.

From the distributions reported in Figure 6 it could be concluded that since the advective momentum transport by the second cross-circulation is not negligible, the core of the maximum downstream velocity is shifted from near the outer bank in the inwards direction.

It should be noted that such result would be restricted to the experimental conditions examined. But, on the basis of literature laboratory studies on cross-circulation (see review in Termini & Piraino, 2011), conducted in curved channel under different hydraulic conditions (and, thus, for different values of *B/h* ratios – but always less than 10),

it could be supposed that the aforementioned effect of the advective momentum transport by the cross-circulation is as more significant as the strength of the counter-rotating circulation cell increases, which makes weak the action of the central circulation cell at the outer bank. This behavior confirms that, in accordance with Blanckaert & Graf (2001), the advective momentum transport by the cross-circulation plays an important role on the bed and outer bank erosion and, thus, on the meander wave morphological evolution. This further highlights the need of an accurate identification of the cross-circulation flow effect.

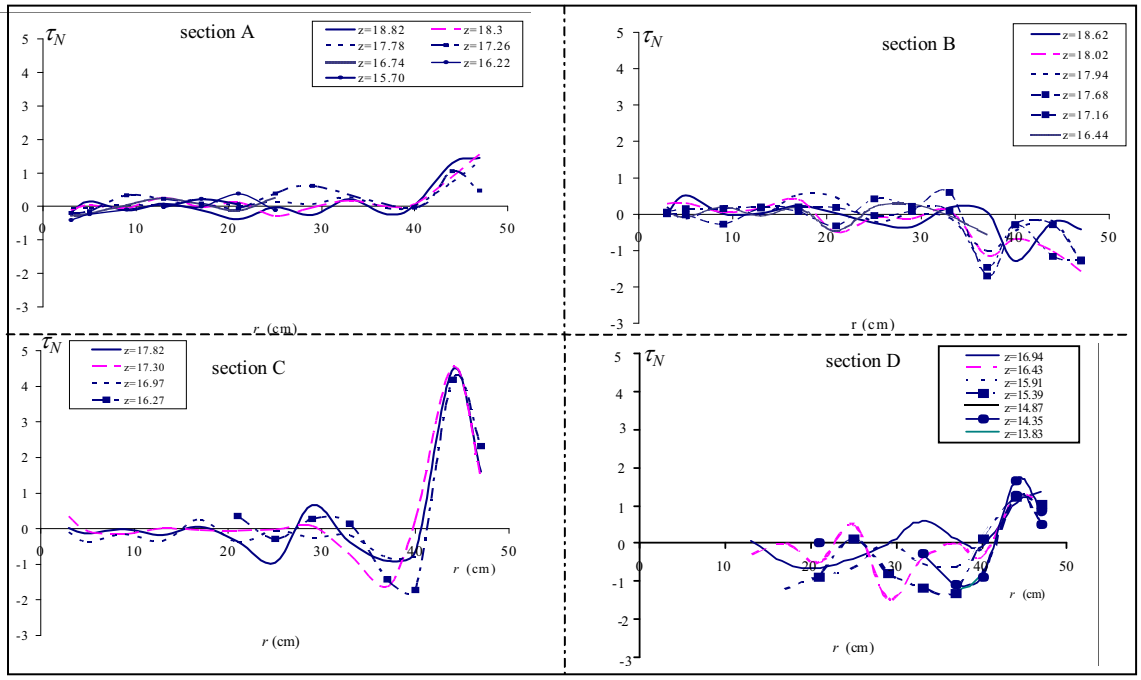

Fig. 5: Horizontal profiles of τ_N .

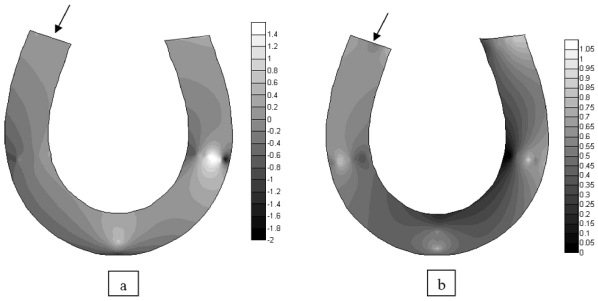

Fig. 6. Map contours: a) normalized depth-averaged streamline function, $<\psi_N>$; b) depth-averaged longitudinal flow velocity $\overline{v_s}$ (m/s)

6. Conclusion

The results presented in this work essentially confirm that, for *B/h*<10, at the bend entrance besides of the central-region circulation cell a counter-rotating circulation cell starts to form near the free surface of the outer bank.

It evolves until to reach the apex section and decays at the bend exit. In the case of B/h>10 it seems that the main central-region circulation cell is not significant, and only at the apex section the outer-bank circulation cell forms. The presence of the outer-bank circulation cell, especially observed in the case of B/h<10, allows the bank shear stress to maintain very low values of close to the bank.

The accurate identification of the cross-circulation effect is strongly related to the accurate identification of the bed topography, which, in turn, depends on the advective momentum transport by the cross-circulation. Since the advective momentum transport by the second cross-circulation is not negligible, the core of maximum downstream velocity is shifted, from near the outer bank, in the inwards direction. Thus, in accordance with Blanckaert & Graf (2001), the advective momentum transport by the cross-circulation plays an important role on the erosion process of the bed and the outer bank and, thus, on the meander wave morphological evolution.

References

Batchelor, G.K. (1967). *An introduction to fluid dynamics*. Cambridge Univ. Press. Cambridge U.K.

Bathurst, J.C.; Thorne, C.R.; Hey, R.D. (1979). Secondary flow nad shear stress at river bends. *Journal of Hydr. Div.* 105(**10**). 1277-1295.

Blanckaert, K.; Buschman, F.A.; Schielen, R.; Wijbenga, J.H.A. (2008). Redistribution of velocity and bed-shear stress in straight and curved open channels by means of a bubble screen laboratory experiments- *J. of Hydr. Eng.*, 134(**2**), 184-195.

Blanckaert, K.; Graf, W.H. (1999). Outer-bank cell of secondary circulation and boundary shear stress in open-channel bends; *I.A.H.R. Symposium on River, Coastal and Estuarine Morphodynamics*; Genova (Italy), September 6-10.

Blanckaert, K.; Graf, W.H. (2001). Mean Flow and Turbulence in Open-channel Bend; *J. of Hydr. Eng.*, 127(**10**), 835-847.

Bradshaw, P. (1987). Turbulent secondary flows. *Annu. Rev. Fluid. Mech*. **19**, 53-74

Dietrich, W.E.; Smith, J.D. (1983). Influence of the point bar on flow through curved channels, *Water Resourc. Res.* 19(**5**), 1173-1192.

Kikkawa, H.; Ikeda S.; Kitagawa, A. (1976). Flow and Bed Topography in Curved Open Channels, *J. Hydr. Div*. - ASCE- 102(**9**), 1327-1342.

Termini, D. (2004). Flow in meandering bends, *International Congress Riverflow*, Napoli 23-25 June, 109-117.

Termini, D.; Piraino, M. (2007). Secondary circulation motion in the apex section of a large amplitude meandering flume, 32nd congress of IAHR, The International Association of Hydraulics Engineering and Research, Venice, 1-7 july.

Termini, D.; Piraino, M. (2008). Experimental investigation of the evolution of secondary motion in a large amplitude meandering flume, *International Congress Riverflow2008*, Izmir-Turkey 3-5 Sept, 1279-1288.

Termini, D.; Piraino, M. (2011). Experimental analysis of cross-sectional flow motion in a large amplitude meandering bend. Earth Surface Processes and Landforms. Vol. 36, issue 2, pp. 244 – 256.

Zimmerman, C.; Kennedy, J.F. (1978). Transverse Bed Slopes in Curved Alluvial Streams, *J. Hydr. Div.*, 104(**1**), 33-48